Geotectonics, Vol. 34, No. 4, 2000, pp. 332–342. Translated from Geotektonika, No. 4, 2000, pp. 85–96.

Cutoff Method for Kinematic Analysis of Faults in Stratified Sequences

A. V. Solov'ev[1] and M. T. Brandon[2]

[1]*Institute of the Lithosphere of Marginal and Inner Seas, Russian Academy of Sciences, Staromonetnyi per. 22, Moscow, 109017 Russia*

[2]*Yale University, 210 Whitney Avenue, P.O. Box 208109, New Haven, USA*

Received April 26, 1999

Abstract—A new kinematic method, cutoff analysis, enables the determination of fault kinematics in stratified sequences. Nappe (thrust) zones formed in a setting of progressive non-coaxial deformation are characterized by monoclinic symmetry. This postulate provides an opportunity to estimate relative transport direction at a regional scale from synoptic stereographic analysis of cutoff structures. The method was applied to two geological sites. The obtained data were similar to those indicated by other fault-kinematic methods. This attests to the truth of our premises and the applicability of the new method to geodynamic reconstructions in various regions. Cutoff structures develop in specific settings, in near-surface stratified sequences resting upon a rigid structural basement, and at considerable deformation rates.

INTRODUCTION

Geodynamic interpretation of geologic structures implies the knowledge of relative transport directions. In geodynamics, these directions are detected from a kinematic analysis of micro- and mesoscale structures referred to as kinematic indicators. The kinematic indicators are rotated porphyroclasts, striation on slickensides, asymmetric folds, Riedel structures, and some other features [11, 14, 17].

The purpose of this paper is to present a new kinematic method referred to as cutoff analysis, which enables one to determine fault kinematics in stratified sequences and to estimate regional stress orientation during their deformation. This method, like the internal rotation axis analysis [14], rests on the principle of symmetry in geologic structures.

The proposed method is applicable primarily to the geologic structures originating from brittle strain at low temperatures (<200°C), the so-called brittle thrusts [14] widespread in the Mesozoic–Cenozoic fold-and-thrust belts of the Pacific Rim and in other regions of the world.

CUTOFF ANALYSIS METHOD

Thrust faulted stratified sequences in various regions often exhibit cutoff structures (Fig. 1a, I, II, III), characterized by fault-parallel bedding in one of the fault walls and an acutely truncated bedding (cutoff) in the other wall. The cutoff method is proposed for the interpretation of fault kinematics. The method is based on a ramp-imbrication model [5, 22] (Fig. 1a). According to this model, compression applied to a stratified sequence under certain conditions gives rise to a fault with a composite configuration, bed-parallel–truncating the bedding–bed-parallel. This fault accommodates the thrusting of hangingwall onto the footwall. Note that the proposed method is only applicable if (1) the sequence is stratified, (2) the movement takes place along a shear plane, and (3) fault plane coincides with a bedding plane in one of the two fault walls.

The available data on natural and model shear zones suggest that the symmetry of all structural elements within these zones is related to the monoclinic deformation symmetry [13, 18, 20]. Therefore, an idealized fault zone initiated in a setting of progressive non-coaxial deformation is characterized by a monoclinic symmetry (Fig. 1b) [14, 23]. The structures that can be described by a duplex model are also characterized by monoclinic symmetry defined by a simple mirror plane (Fig. 1a). This plane can be inferred from the geometry and asymmetry of structural features, and slip direction is defined as the intersection of the plane of symmetry and fault plane.

During field surveys of real exposures, cutoff structures were observed both in hangingwalls (Fig. 1a, I) and in footwalls (Fig. 1a, II). Slip direction is determined from the relationship between stratigraphic sequences in the hangingwall and footwall. The fault truncates bedding moving from the older to younger sediments in the hangingwall (Fig. 1a, I) and, vice versa, in the footwall (Fig. 1a, II). A specific case, also observed in real exposures, is the overturned bedding in the hangingwall (Fig. 1a, III), but, even in this case, the rule for the hangingwall remains valid. Actually, the discussed structures bear evidence for the rotational component of movement; therefore, the orientation and asymmetry of these structures can be described by an

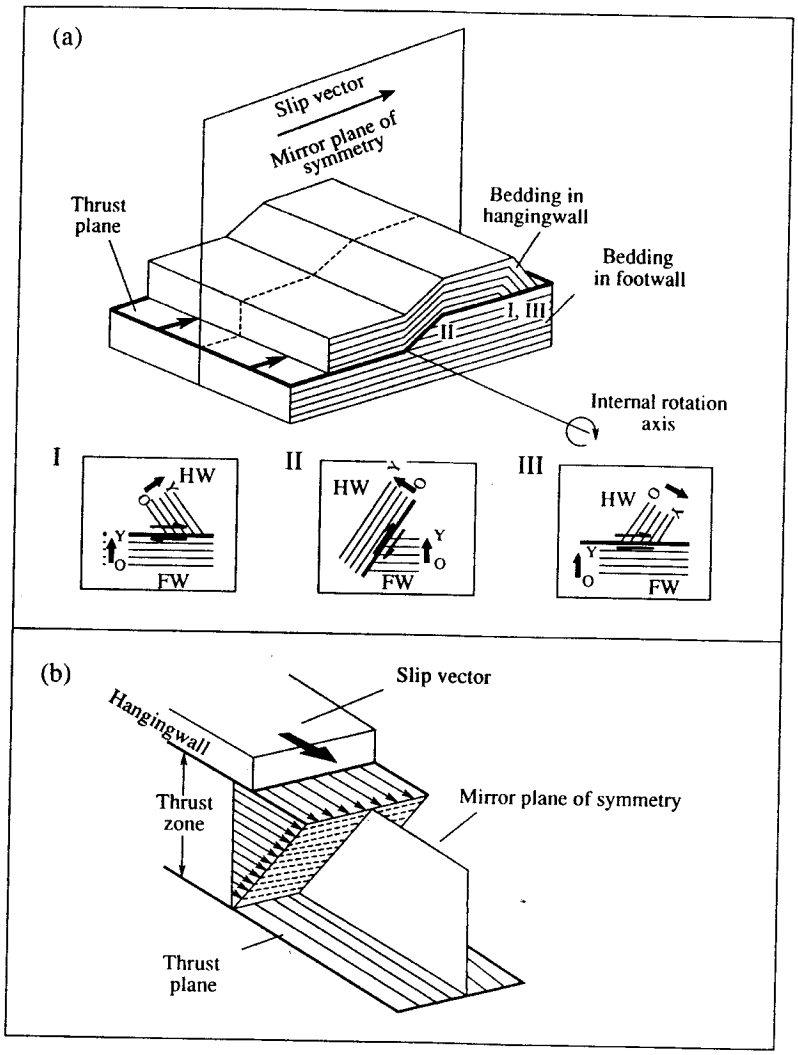

Fig. 1. (a) An idealized model of a duplex structure (modified after [22]). The model is adapted for the cutoff analysis method. I, II, and III are the possible bedding combinations in the hangingwall (HW) and footwall (FW). Faults are shown by solid lines. Arrows indicate the stratigraphic sequence from the older (O) to younger (Y) sediments. See the text for explanations. (b) An idealized chart of a thrust zone with monoclinic symmetry formed in a setting of progressive non-coaxial deformation [14, 23].

internal rotation axis (Fig. 1a) by analogy with the internal rotation axis analysis [14]. This axis is an axial vector, indicating the sense of rotation, which can be designated as either "Z" or "S" rotation. Z-rotation is clockwise, and S is anticlockwise, when viewed in the direction indicated by the axial vector. Z and S are equivalent to "right-handed" and "left-handed" rotations, where the thumb is extended in the direction of the axis, and the remaining fingers curl in the direction of rotation.

To summarize, the slip vector of a particular cutoff structure is determined by measuring the fault plane and the cutoff bedding plane orientations and the subsequent calculation of their intersection line, the internal rotation axis. The local slip vector lies in the fault plane and is orthogonal to the internal rotation axis. However, the available data on regional fault zones [8, 14] suggest that the orientations of structures within them are widely varying. Consequently, the regional transport vector should be determined by the average of numerous cutoff measurements.

The regional (synoptic) internal rotation axis and the regional (synoptic) slip vector are calculated using the algorithm previously suggested for the internal rotation axis analysis [14]. A stereogram (Schmidt net) of local internal rotation axes is plotted. The fault plane is defined as the great-circle (average) girdle, along which local rotation axes are dispersed. The mirror plane of symmetry bisects the features with S and Z symmetries into two groups and is orthogonal to the average fault plane and perpendicular to a maximum of local rotation axes. The maximum of local rotation axes corresponds to the maximum value of the eigenvector that describes the distribution of these axes and repre-

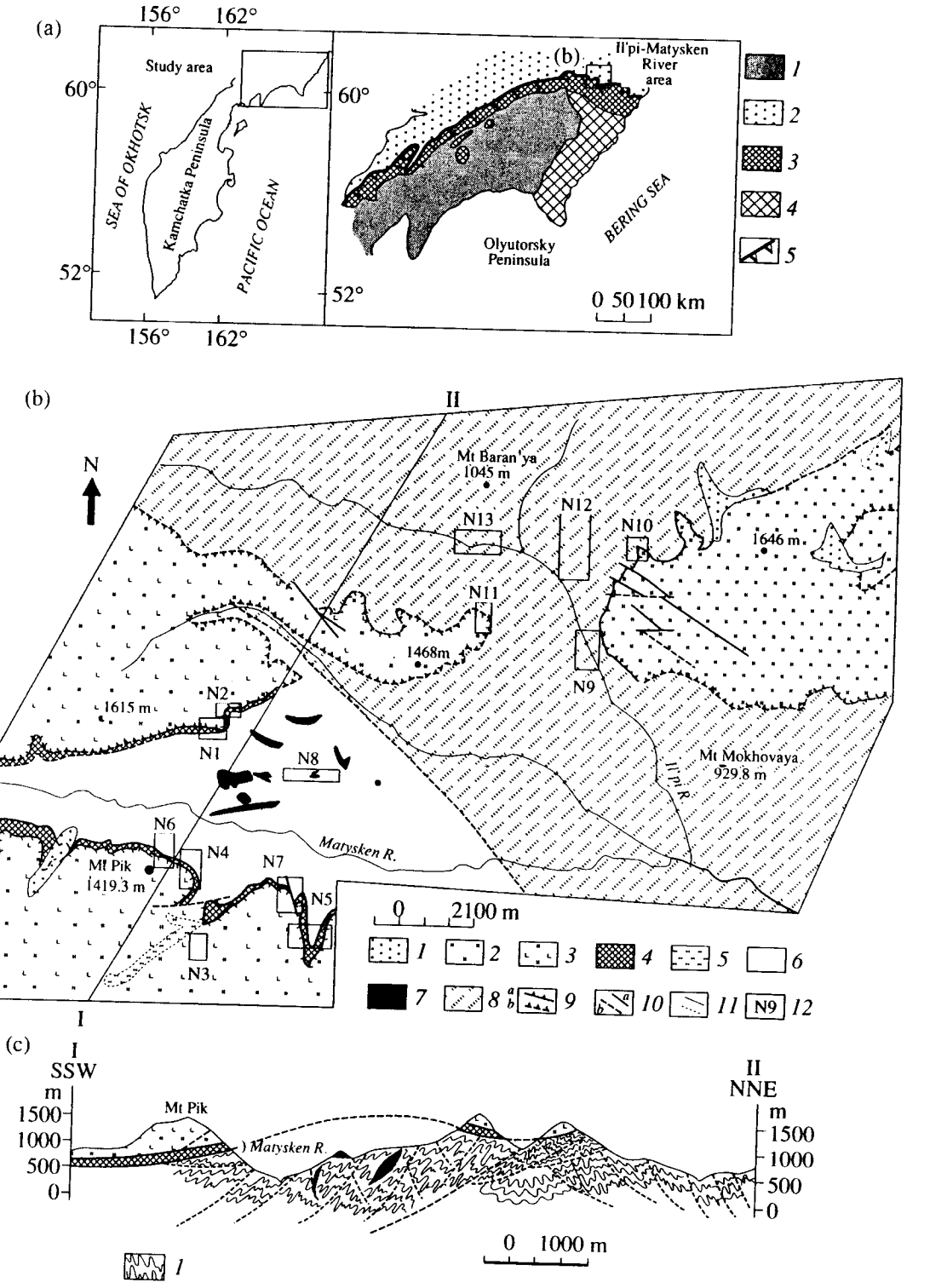

Fig. 2. Geologic structure of the area in the upper reaches of the Il'pi and Matysken rivers. (a) Location of the study area at the junction of the Ukelayat and Olyutorsky zones: (*1*) Cenozoic sediments; (*2*) Cretaceous–Paleogene deposits of the Ukelayat zone; (*3*, *4*) Cretaceous deposits of the Olyutorsky zone: (*3*) frontal zone, (*4*) Olyutorsky Range; (*5*) Vatyna–Vyvenka thrust. (b) Draft geologic map of the area in the upper reaches of the Il'pi and Matysken rivers (compiled with the aid of G.V. Ledneva and J.I. Garver using data of A.V. Ditmar, K.S. Ageev, A.S. Finogentov, and E.S. Alekseev). (*1*) Loose Quaternary sediments; (*2*, *3*) volcanic–cherty deposits: (*2*) chert, jasper; (*3*) aphyric pillow basalt, chert, jasper; (*4*) Vatyna–Vyvenka thrust zone; (*5*) dunite, vehrlite, and clinopyroxenite blocks; (*6*) olistostrome sequence; (*7*) blocks of basaltic rocks; (*8*) Ukelayat flysch; (*9*) thrusts: (*a*) proved, (*b*) inferred; from aerial image interpretation (*10*) high-dipping faults: (*a*) proved, (*b*) inferred; (*11*) contacts: (*a*) proved, (*b*) inferred; (*12*) numbers of the domains, in which structural observations were conducted. (c) Generalized cross section I (SSW)–II (NNE). See Fig. 2b for the legend except (*1*), folding in the autochthon.

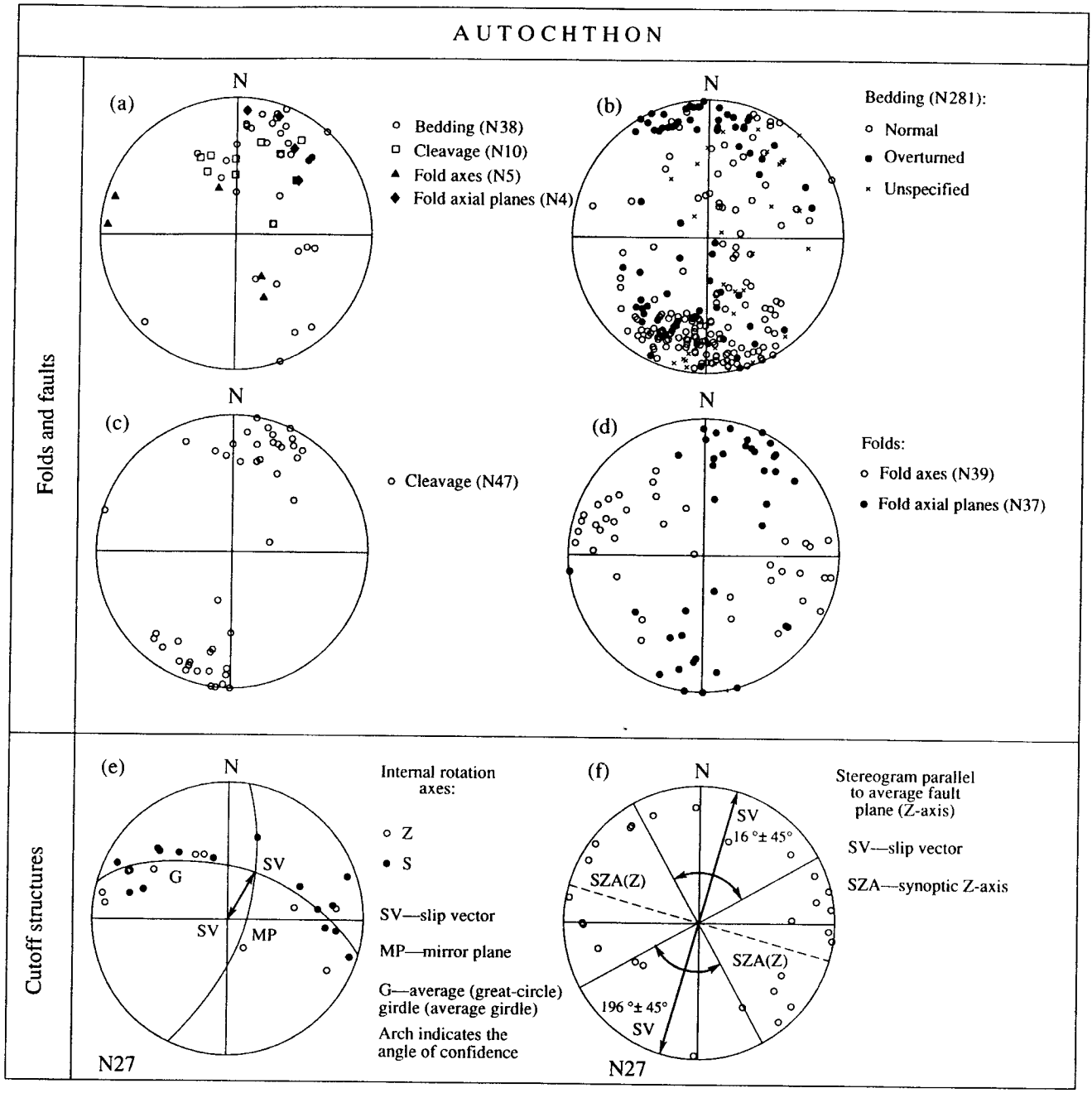

Fig. 3. Structural-kinematic data on the flyschoid rocks of the Ukelayat zone (the Il'pi–Matysken River area). All structural features are plotted on a Schmidt net, projection into the lower hemisphere. N is the number of structural features of the type plotted on a given stereogram. The orientations of planar structural features (bedding, cleavage, axial planes of folds) are shown as pole (normal) orientations, and the orientations of the linear structural features (fold and rotation axes) are given according to their dip and inclination. Stereograms of various structural features in domains *1–8* (a) (see Fig. 2) and *9–13* (b–d): (b) bedding poles; (c) cleavage; (d) axes and poles of the axial planes of folds; (e) stereogram of the internal rotation axes of cutoff structures; (f) Z-transformed rotation axes projected onto the average fault plane.

sents an estimated synoptic internal rotation axis in modern coordinates. The azimuth of slip vector in fault plane is estimated using the following procedure. All local cutoff structures with S-symmetry are inverted into Z-axes. For instance, the S-axis, projected into the upper hemisphere to be inverted into a Z-axis, will be mirror-reflected in the lower hemisphere. Then, the Z-transformed axes are projected into the "average" fault plane. The resulting diagram is called a fault-parallel stereogram. The maximum of Z-transformed axes distribution represents the synoptic rotation axis in the "average" fault plane, and the synoptic (regional) vector of hangingwall motion relative to the footwall lies orthogonally to that axis in the same plane. Some spe-

Table 1. Planar element orientations in cutoff structures, estimated local interior rotation axes, and slip vectors (flyschoid deposits in the upper reaches of the Il'pi River)

Wall[1]	Bedding orientation		Normal/overturned[2]	Fault plane orientation		Normal/overturned[3]	Internal rotation axis		Angle[4]	Slip vector	
	AD	A		AD	A		D	I		D	I
F	179	84	O	203	51	O	86	−30	40	150	+37
F	338	45	N	351	40	O	202	−36	10	280	+16
F	349	34	N	357	20	N	250	−6	14	338	+19
H	10	68	N	42	40	N	266	−31	38	341	+22
H	260	62	N	342	40	N	145	−39	64	242	−9
H	002	65	N	205	85	O	111	−36	37	302	−54
H	207	58	O	007	80	N	281	+23	46	75	+64
H	030	73	N	174	68	O	105	+41	53	244	+41
H	162	74	O	018	75	N	271	−48	48	300	+38
H	220	50	O	158	82	O	239	−48	64	75	−42
H	020	75	N	010	52	N	295	+19	25	46	+46
H	**080**	**53**	**N**	**010**	**71**	**N**	**74**	**+53**	**63**	**116**	**−38**
H	000	54	N	320	57	N	349	+54	33	59	−14
F	165	72	N	355	82	O	262	−21	28	64	−69
H	020	52	N	005	65	N	75	+36	18	121	−43
H	042	68	N	030	58	N	332	+40	15	99	+30
H	260	46	N	019	58	N	132	−32	86	135	−53
H	019	57	N	008	49	N	317	+36	12	70	+28
F	015	65	N	018	57	N	277	−16	8	32	+56
H	357	52	N	019	57	N	163	−51	19	317	−36
H	025	56	N	035	70	N	136	−28	17	342	−55
H	019	55	N	025	80	N	117	−11	26	337	−75
H	**243**	**70**	**O**	**021**	**70**	**N**	**312**	**+45**	**33**	**94**	**+39**
F	200	86	N	020	74	O	290	0	70	200	−74
H	105	77	N	065	89	N	152	+71	41	155	−19
F	012	83	O	008	54	O	283	+7	29	202	−53
F	318	52	N	006	28	N	105	−27	38	302	+13

Note: AD—dip azimuth and A—dip angle of a planar element; D—dip and I—inclination of an axis or vector. Positive dip is the projection of a direction into the lower hemisphere; negative, into the upper hemisphere. [1] F—footwall; H_hangingwall; [2] dip of bedding in the cutoff wall, N—normal and O—overturned; [3] dip of fault-parallel bedding; [4] angle between the fault plane and cutoff surface. Slip vector (for local structures) was calculated as the intersection of the fault plane and the plane orthogonal to internal rotation axis. The data on the structures used in Figs. 4a–4d are given in bold.

cific features of synoptic rotation axes and vectors estimation procedure will be discussed in the description of the method as applied to regional objects.

TESTING OF THE METHOD: REGIONAL CASES

We have tested the possibilities of the proposed method on two terranes: (1) the flyschoid sequence of the Ukelayat zone in the southern Koryak Highland [12] and (2) the flysch of the Tauria Group, exposed on the southern coast of Crimea [2, 19].

Structures of the Flyschoid Complex of the Ukelayat Zone

The Ukelayat zone in the southern Koryak Highland separates the structures of the Olyutorsky zone from the accretionary complexes of the Koryak Highland to the north (Fig. 2a). The flyschoid sequence of the Ukelayat zone was formed during the Cretaceous–Paleogene along the Eurasian continental margin [6, 9]. The deposits of the Ukelayat zone are strongly deformed.

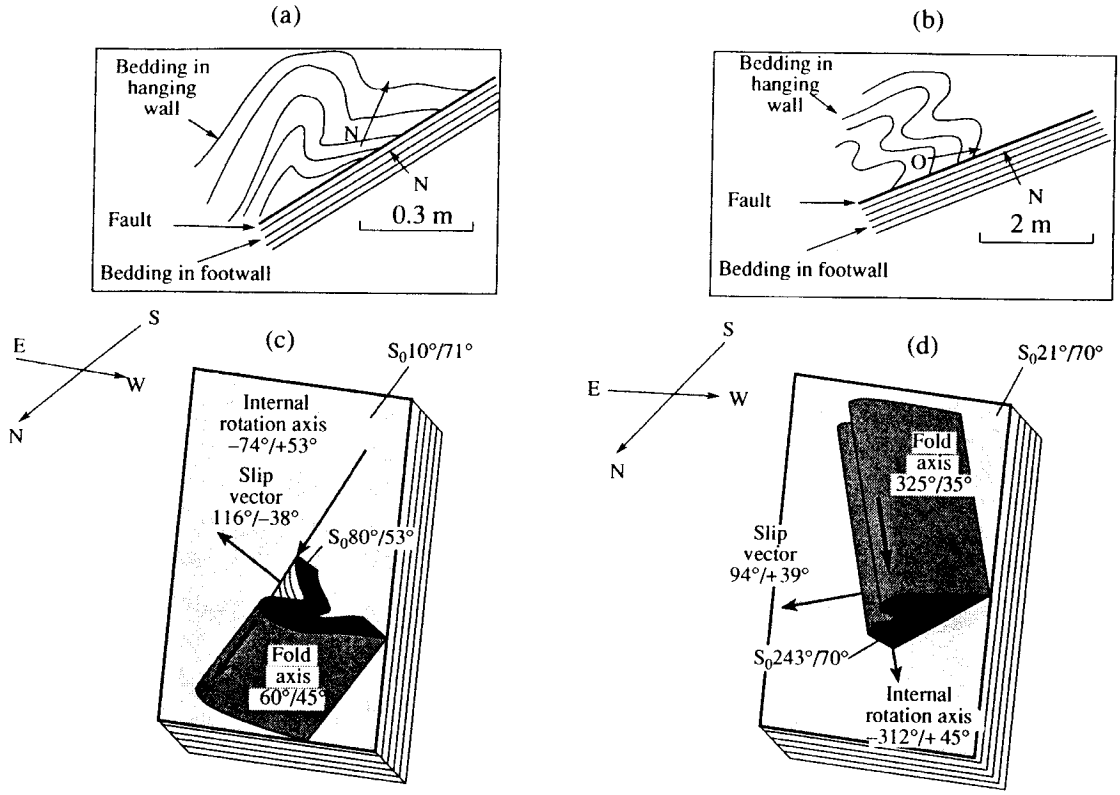

Fig. 4. Two types of kinematic indicators, asymmetric folds, and cutoff structures. (a), (b) Sketches of natural outcrops (N—normal bedding, O—overturned bedding). (c), (d) Block diagrams of relationships among asymmetric folds and cutoff structures (bedding attitudes S_0 and fold axes were measured in natural outcrops; internal rotation axes and slip vectors, calculated (see Table 1 in bold).

Our structural investigations were conducted along the southern margin of the Ukelayat zone, where the allochthonous complexes of the Olyutorsky zone rest on the autochthonous Ukelayat flysch along the Vatyna–Vyvenka thrust fault (Fig. 2b). The autochthon is a flyschoid sequence of thinly interbedded sandstones, siltstones, and mudstones with occasional gritstones and conglomerates. In the Il'pi and Matysken river valleys (Fig. 2b), a strongly tectonized sequence of presumably olistostrome origin was described at the top of the autochthonous flysch. The matrix is composed of black aleuropelites with occasional thin sandstone layers. The blocks are composed of porphyritic or aphyric basalts, basaltic lava-breccias and hyaloclastites, gabbroids and gabbro–diorites, and occasional black and green cherts [10]. The zircon fission-track age of the sequence is Late Maastrichtian–Middle Eocene (66.1 ± 6.3 to 43.9 ± 3.6 Ma) [9, 15, 16].

In the Il'pi–Matysken area, the autochthon shows a regular distribution of fold vergence orientations (Figs. 2b, 2c). Within distance from the thrust fault, the northward vergence of the olistostrome sequence exposed near the Vatyna–Vyvenka thrust fault (Fig. 3a and domains 1–8 in Fig. 2b) first grades into a fan folding zone and then into a zone with south-southwestward vergence (domains 9–13 in Fig. 2b, Fig. 3b). Within domains 9–13, the axial planes of folds dip NNE as well as SSW (Fig. 3d), and fold axes show a west-northwestward and east-southeastward dip at low angles (Fig. 3d) and an axial-plane cleavage (Fig. 3c). Analysis of all structural features of the autochthonous complex within the study area suggests that they were formed in a stress field with a SSW–NNE orientation of the main compression axis [8].

Cutoff structures are widespread in the autochthonous flysch, and this enabled us to test the proposed method on a terrane, where the obtained data could be checked by standard structural methods. Twenty-seven cutoff structures were studied in the olistolith-free flysch zone (domains 9–13, Fig. 2b; Table 1). All possible relationships between faults and bedding, shown in Fig. 1 I–III, were observed in outcrops. Internal rotation axes were estimated from the field measurements of the attitudes of bedding planes and the faults that truncated them (Table 1). Local slip vectors were calculated as the intersections of the planes orthogonal to the internal rotation axis and the fault planes. In two cases, cutoff structures were observed together with some other kinematic indicators, asymmetric or drag folds (Figs. 4a, 4b). In the former case, a Z-asymmetric fold was detected in the hangingwall of a cutoff structure (axis oriented at 60°, 45°), indicative of a southeastward slip. The internal rotation axis, calculated from the cutoff structure, was closely similar to the asym-

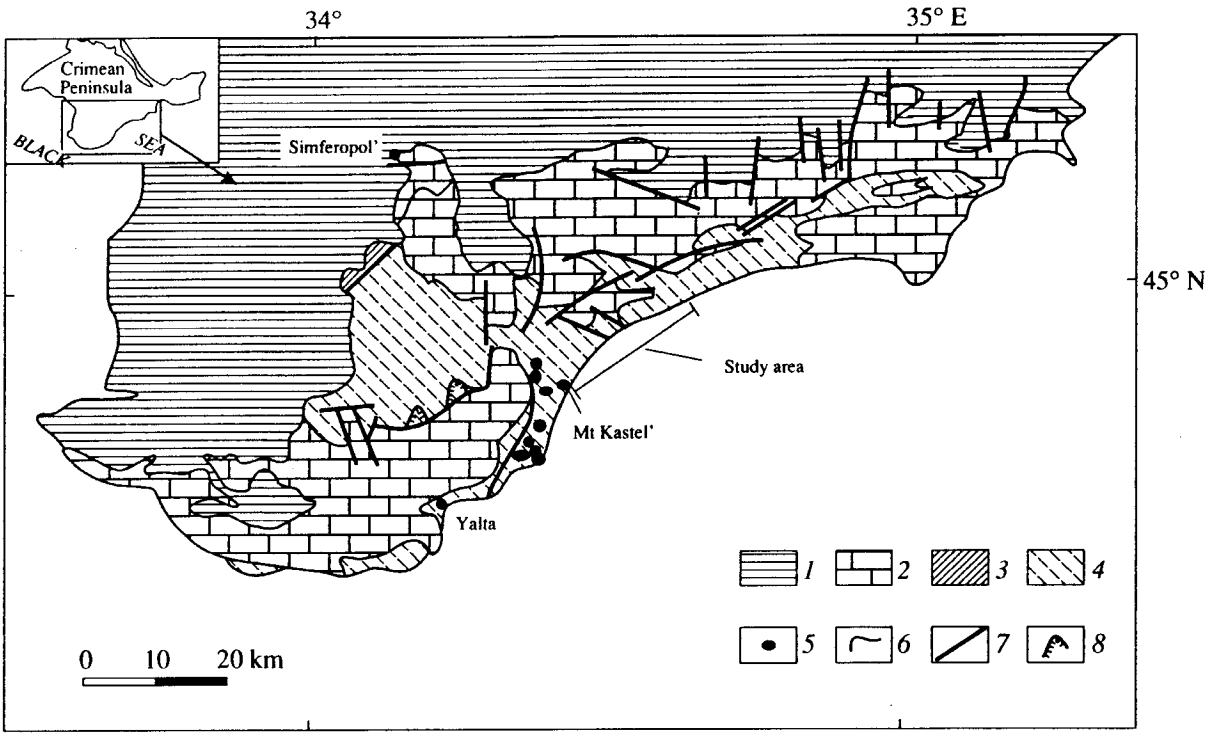

Fig. 5. Draft geologic map of the Crimean Mountains [2]. (*1*) Cretaceous–Neogene and (*2*) Upper Jurassic deposits; (*3*, *4*) Middle Triassic–Middle Jurassic Crimean sequence: (*3*) Eskiorda and Karadag groups and (*4*) Tauria Group; (*5*) Bajocian intrusions; (*6*) geologic boundaries; (*7*, *8*) faults: (*7*) normal and reverse faults and (*8*) thrusts.

metric fold axis (oriented at 74°, 53°) and enabled the estimation of a southeastward slip vector (116°, 38°) (Fig. 4c). In the latter case, the asymmetric fold axis is also similar to the internal rotation axis of the cutoff structure (Fig. 4d). To summarize, the cutoff structures are good kinematic indicators as is obvious from comparison with the other structures enabling the estimation of slip directions.

Regional paleostress directions are reconstructed from the analysis of internal rotation axes distribution for local structures (Table 1). The estimated internal rotation axes are dispersed along a great-circle girdle (Fig. 3e) as is typical of fault zones with a monoclinic symmetry [14]. The great circle defines the "average" fault plane (16°, 58°). The S and Z axes show a mixed distribution, which suggests that the faults accommodated both north-northeastward and south-southwestward motions. The synoptic (regional) slip vector can be estimated by two methods. Firstly, the synoptic vector can be calculated as the mean of the slip vectors for local structures (Table 1). The estimates for two opposite vectors will be 11° ± 35° and 191° ± 35°. Secondly, the synoptic internal rotation axis and slip vector can be calculated using the algorithm described above [14]. This method yields vector estimates of 16° ± 45° and 196° ± 45° (Fig. 3f). Although the vector estimates obtained by the first and second methods are closely similar, we prefer the second estimate, because it takes into account the monoclinic symmetry of the fault zone and provides a better averaging of random variations.

Thus, the estimated slip vectors (Fig. 3f) suggest that intraformational thrusting of the Ukelayat flysch took place in the north-northeastern as well as south-southwestern directions, giving rise to a fan-shaped vergence pattern. The reliability of the data obtained by cutoff analysis method is supported by independent structural data as mentioned above. Note that the proposed method enables a quantitative estimation of regional slip vectors and the confidence intervals of the obtained values.

Structures of the Tauria Flysch (South Crimea Coast)

The Tauria Group is a Middle Triassic–Middle Jurassic sequence exposed in the Crimea Peninsula (Fig. 5). The deposits of this sequence are strongly deformed and occupy the lowermost structural position. The Tauria Group consists of a flyschoid sequence of interbedded sandstones, siltstones, and mudstones of Late Triassic–Middle Jurassic age [2, 19]. The base of the group is not exposed anywhere in Crimea, and the relationship with the underlying strata is unknown. The Tauria Group is discordantly overlain by the Upper Jurassic in the southern and eastern parts of the Kacha high and by the Lower Cretaceous, in the north and west. The Tauria Group consists of proximal and distal turbidites accumulated in a basin, which separated the

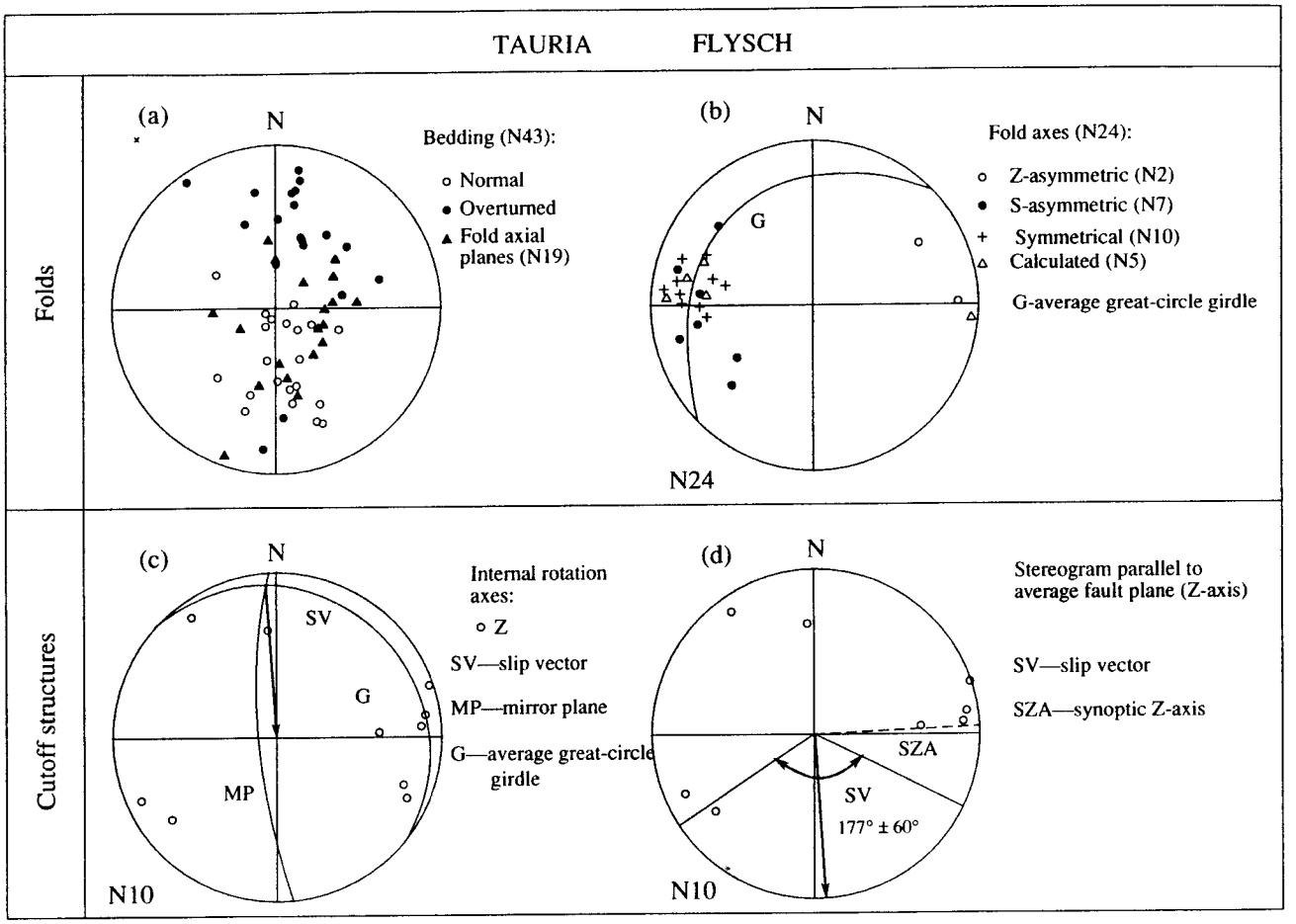

Fig. 6. Structural-kinematic data on the flyschoid rocks of the Tauria Group (southern Crimea coast, see Fig. 5). All structural features are plotted on a Schmidt net, projection into the lower hemisphere. N is the number of structural features of the type plotted on a given stereogram. The orientations of planar structural features (bedding, cleavage, axial planes of folds) are shown as pole (normal) orientations, and the orientations of the linear structural features (fold and rotation axes) are given according to their dip and inclination. Stereograms (a–c) of (a) bedding poles and axial planes of folds; (b) fold axes; (c) internal rotation axes for cutoff structures; (d) Z-transformed rotation axes projected onto the average fault plane. SV—slip vector; the arc indicates the angle of confidence.

Scythian platform and the Euxinia terrane during Late Triassic–Middle Jurassic time [19].

The studies of the structural style of the Tauria Group were accomplished on the South Crimea coast between the Semirech'e village and Mount Kastel' (Fig. 5). The flysch is deformed into south to southeast-vergent folds; sequences with normal bedding are predominantly north-dipping, and those with overturned bedding are south-dipping (Fig. 6a). There are occasional isoclinal recumbent folds. The axial planes of folds are northwest to north-dipping (Fig. 6a). Fold axes are roughly E–W-trending and shallow-dipping (Fig. 6b). Asymmetric and drag folds are indicative of a south-southwestward transport of the structurally higher part of the group relative to its lower part (Fig. 6b). In addition to asymmetric folds, the flysch exhibits cutoff structures (Table 2). The calculated internal rotation axes of the cutoff structures are dispersed along a great-circle girdle on a stereogram (Fig. 6c) as is typical of deformation zones with a monoclinic symmetry. The great circle represents the average fault plane (41°, 13°). Z-axes are clustered in the eastern sector, and this is indicative of a southward transport along intraformational thrust planes. The synoptic vector, determined as the average for the slip vectors of local structures (Table 1) in the average fault plane is estimated as 171° ± 47°. The synoptic slip vector azimuth calculated as perpendicular to the synoptic rotation axis in the average fault plane is 177° ± 60° (Fig. 6d). The vector azimuths estimated by the first and second methods are closely similar, but we prefer the second estimate.

Cutoff analysis data suggest that the hangingwalls of intraformational thrust faults in the Tauria Group moved southward. This conclusion is supported by other structural data (Figs. 6a, 6b), e.g., asymmetric and drag folds (Fig. 6b), which are widely used as kinematic indicators.

Table 2. Planar element orientations in cutoff structures, estimated local interior rotation axes, and slip vectors (Tauria Group, southern Crimea coast)

Wall[1]	Bedding orientation		Normal/overturned[2]	Fault plane orientation		Normal/overturned[3]	Internal rotation axis		Angle[4]	Slip vector	
	AD	A		AD	A		D	I		D	I
H	225	40	N	270	20	N	111	−19	29	199	+7
H	40	46	N	325	40	N	355	+36	49	74	−15
F	285	32	N	244	21	N	232	+21	21	341	−3
F	250	39	N	220	49	N	88	−38	23	155	+26
H	200	29	N	188	47	N	86	−13	19	163	+44
H	230	12	N	313	16	N	82	−10	19	174	−12
H	14	49	N	22	73	N	116	−14	25	221	−46
H	165	51	O	176	15	N	72	+4	36	161	+15
H	165	47	N	183	22	N	245	+11	27	144	+45
F	350	13	N	287	15	N	325	+12	15	53	−9

Note: See Table 1.

DISCUSSION

Our experience suggests that cutoff structures, quite frequent in the deformed stratified sequences of some regions, may be missing or scarce in similar complexes in other regions. According to previous concepts, thrusts develop in stratified sequences in a setting of horizontal compression when the longitudinal shortening cannot be any more compensated by folding [1]. However, recent investigations, including physical and mathematical structural modeling and field data, suggest that thrusts (a particular case of cutoff structures) may not only arise at a general compression stage. Strain is likely to show itself as cutoff structures in certain specific conditions. Among them are (1) rock lithology, (2) P–T conditions (i.e., the structural depth of deformation), (3) deformation rate, and (4) basement characteristics. Depending on the relations among these four conditions, the strain will be realized either as buckle folding or as shear-related thrusting.

Lithology. The capability of a stratified sequence to deform in a certain way depends on its lithology [7]. For instance, "modeling data suggest that certain combinations of parameters such as the viscosity difference between adjacent layers, their capability to slip along each other, or their thicknesses may facilitate thrusting as an energetically viable process even at the initial deformation stages. This may give rise to blind thrusts in stratified sequences, whose thrust planes do not reach the surface and die out in a low-viscosity layer or at a interformational slip surface" [3, p. 11]. Thus, modeling and natural observations indicate that cutoff structures are a frequent form of strain realization in stratified (flyschoid) sequences. Another important lithological parameter of a stratified sequence is the state of rocks, i.e., the extent of lithification, which directly depends on P–T conditions experienced by the sequence.

P–T conditions (structural depth of deformation). Brittle thrust deformations in stratified sequences may only take place after diagenesis and at low temperatures (<200°C) and pressures, i.e., near the surface. This premise is supported by the absence of significant metamorphic alterations in the Ukelayat and Tauria flyschoid sequences. The flysch sandstones from the Ukelayat zone (see above) show almost no signatures of pressure-solution cleavage [21]. Detrital zircons, extracted from the Ukelayat sandstones, had never been heated above ~180–240°C after the deposition in the basin as obvious from fission-track dating data [9, 15, 16]. Detrital apatites from the same rocks were heated to a temperature of ~60–120°C after deposition [16]; therefore, the structural thickness of the overburden did not exceed ~3–4 km in case of a normal temperature gradient (25°C/km). The aforementioned direct and indirect data suggest that the cutoff structures are formed predominantly near the surface at low temperatures and pressures.

Deformation rate. Brittle deformations prevail over folding at high rates of geological processes. The examples discussed in this article refer to the regions with active geodynamics. The deposits of the Ukelayat zone were deformed in a zone of convergent oceanic and continental lithosphere, and the absence of pronounced pressure-solution cleavage [21] attests to a high deformation rate during structure formation in the Ukelayat zone.

Basement characteristics. The physical modeling of deformation in stratified sequences shows that the probability of thrusting largely depends on the presence of rigid basement at the base of the sequence [3]. The

rigid basement prevents from folding as it disables the formation of synclines necessary for the compensation of adjacent anticlines [4]. "In a sequence resting upon a basement and consisting of beds with different viscosities, plastic buckling of folds may give way to the formation of blind thrusts in its lower parts" [3, p. 12]. Actually, any rocks with an overall viscosity higher than that of the overburden may serve as the rigid basement. In our case, the Ukelayat flysch was formed on the continental rise and on slope terraces, and the nature of deformations was guided by the presence of a rigid continental basement.

To summarize, the presence of cutoff structures in a stratified sequence implies that they were formed in specific conditions, near the surface, at a considerable deformation rate, and upon a rigid structural basement.

CONCLUSIONS

(1) Cutoff analysis method enables one, with certain allowances, to reconstruct fault kinematics in stratified sequences, and the array measurements of cutoff structure attitudes and their subsequent statistical analysis enable one to estimate regional transport direction.

(2) The testing of cutoff analysis method on two geological sites yielded data comparable with those obtained by other structural-kinematic methods. This attests to the truth of our premises and enables us to apply the method to geodynamic reconstructions in various regions.

(3) Cutoff structures are formed in stratified sequences with contrasting viscosities of constituent beds and a capability of these beds to slip along each other. These structures form in diagenetically consolidated rocks at low temperatures (<200°C) and pressures. Thrusting prevails over folding at considerable deformation rates. The inception of trusting largely depends on the presence of a rigid basement beneath the sequence.

ACKNOWLEDGMENTS

We are grateful to G.V. Ledneva and J.I. Garver for the assistance in field surveys and to our reviewers, V.S. Burtman and A.V. Luk'yanov, whose critical remarks facilitated the improvement of the manuscript.

This work was supported by the Russian Foundation for Basic Research (project no. 98-05-64525) and NSF EAR (projects nos. 94-18989 and 94-18990).

REFERENCES

1. Belousov, V.V., *Strukturnaya geologiya* (Structural Geology), Moscow: Nedra, 1986.
2. *Geologicheskoe stroenie Kachinskogo podnyatiya Gornogo Kryma. Stratigrafiya mezozoya* (Geologic structure of the Kacha High in the Crimean Mountains: Mesozoic stratigraphy), Mazarovich, O.A. and Mileev, V.S., Eds., Moscow: Mosk. Gos. Univ., 1989.
3. Golev, M.B., Physical Modeling of the Process of Thrusting in Bedded Sequences under Horizontal Compression, *Geologicheskie issledovaniya litosfery* (Geologic Surveying of the Lithosphere), Moscow: In-t Litosfery RAN, 1995, pp. 11–12.
4. Goncharov, M.A., Compensation-Related Organization of Tectonic Flow and Structural Associations, *Geotektonika*, 1993, no. 4, pp. 19–29.
5. Goncharov, M.A. and Frolova, N.S., Computer Modeling of Nappe Formation Process, *Vestn. Mosk. Univ., Ser. 4: Geol.*, 1995, no. 3, pp. 49–60.
6. Ermakov, B.V. and Suprunenko, O.I., Structure and Depositional Environment of the Late Cretaceous and Miocene Flysch in the Koryak–Kamchatka Region, *Sov. Geol.*, 1975, no. 12, pp. 53–65.
7. *Metody modelirovaniya v strukturnoi geologii* (Modeling Methods in Structural Geology), Moscow: Nedra, 1988.
8. Solov'ev, A.V., Geologic Structure and Kinematics of the Vatyna-Vyvenka Nappe (Koryak Highland), *Abstract of Cand. Sc. (Geol.–Min.) Dissertation*, Moscow: 1997.
9. Solov'ev, A.V., Brandon, M.T., Garver, J. I., Bogdanov, N.A., Shapiro, M.N., and Ledneva, G.V., Collision between the Olyutorskiy Island Arc and the Eurasian Continental Margin: Kinematic and Timing Aspects, *Dokl. Akad. Nauk*, 1998, vol. 360, no. 5, pp. 666–668.
10. Solov'ev, A.V., Palechek, T.N., and Ledneva, G.V., The Campanian–Maastrichtian Deposits at the Front of the Olyutorskiy Zone (Southern Koryak Highland), *Stratigr. Geol. Korrelyatsiya*, 2000, vol. 8, no. 2, pp. 71–79.
11. Angelier, J., Tectonic Analysis of Fault Slip Data Sets, *J. Geophys. Res.*, 1984, vol. 89, pp. 5835–5848.
12. Bogdanov, N.A., Til'man, S.M., and Chelhovich, V.D., Late Cretaceous–Cenozoic History of the Koryak–Kamchatka Region and the Commander Basin of the Bering Sea, *Intern. Geol. Rev.*, 1990, vol. 32, no. 12, pp. 1185–201.
13. Chester, F.M. and Logan, J.M., Composite Planar Fabric of the Gouge from the Punchbowl Fault, California, *J. Struct. Geol*, 1987, vol. 9, pp. 621–634.
14. Cowan, D.S. and Brandon, M.T., A Symmetry-Based Method for Kinematic Analysis of the Large-Slip Brittle Fault Zones, *Am. J. Sci.*, 1994, vol. 294, pp. 257–306.
15. Garver, J.I., Bullen, M.E., Brandon, M.T., Soloviev, A.V., Ledneva, G.V., and Bogdanov, N.A., Age and Thermal History of the Ukelayat Flysch and Its Bearing on the Timing of Collision of the Olutorsky Terrane, Northern Kamchatka, Russian Far East, *6th International Zoneshain Conference: Moscow, Russia*, Moscow, 1998, pp. 173–174.
16. Garver, J.I., Bullen, M.E., Brandon, M.T., and Soloviev, A.V., Source of Ukelayat Flysch and Collision of the Olutorsky Arc, Northern Kamchatka, Russian Far East, *GSA. Abstracts with Programs*, 1998, vol. 30, no. 7, p. 296.
17. Hancock, P.L., Brittle Microtectonics: Principles and Practice, *J. Struct. Geol*, 1985, vol. 7, pp. 437–457.
18. Logan, J.M., Friedman, M., Higgs, N., Dengo, C., and Shimamoto, T., Experimental Studies of Simulated Gouge and Their Application to Studies of Natural Fault Zones, *Proc. of Conference VIII on Analysis of Actual Fault Zones in Bedrock: U.S. Geological Survey. Open-File Report 79-1239*, 1979, pp. 305–343.

19. Mileev, V.S. and Rozanov, S.B., The Structure and Tectonic Evolution of the Mountain Crimea, *5th Zonenshain Conference on Plate Tectonics: Program and Abstracts*, Moscow: GEOMAR, 1995, p. 81.

20. Morgenstern, N.R. and Tchalenko, J.S., Microscopic Structures in Kaolin Subjected to Direct Shear, *Geotechnique*, 1967, vol. 17, pp. 309–328.

21. Rumthun, A., Brandon, M.T., and Ring, U., Fabric Analysis in the Ukelayat Flysch in the Footwall of the Vatyna Thrust Zone, Kamchatka, Russia: Sedimentary or Tectonic Fabrics? EUG9. Abstract. Supplement no. 1, *Terra Nova*, 1997, vol. 9, p. 377.

22. Suppe, J., *Principles of Structural Geology: Englewood Cliffs*, London: Prentice-Hall, 1985.

23. Twiss, R.J. and Gefell, N.J., Curved Slickenfiber: A New Brittle Shear Sense Indicator with Application to a Sheared Serpentinite, *J. Struct. Geol.*, 1990, vol. 12, pp. 471–481.

Reviewers: V.S. Burtman and A.V. Luk'yanov